Advanced Composite Materials
Publication details, including instructions for authors and subscription information:
http://www.tandfonline.com/loi/tacm20

Analytical methods for prediction of tensile properties of plain knitted fabric reinforced composites

S. Ramakrishna [a], Z. Maekawa [b] & N.K. Cuong [c]

[a] Department of Mechanical and Production Engineering, Faculty of Engineering, The National University of Singapore, 10 Kent Ridge Crescent, 119260 Singapore

[b] Department of Polymer Science and Engineering, Faculty of Textile Science, Kyoto Institute of Technology, Matsugasaki, Sakyo-ku, Kyoto 606, Japan

[c] Department of Polymer Science and Engineering, Faculty of Textile Science, Kyoto Institute of Technology, Matsugasaki, Sakyo-ku, Kyoto 606, Japan

Version of record first published: 02 Apr 2012.

To cite this article: S. Ramakrishna , Z. Maekawa & N.K. Cuong (1997): Analytical methods for prediction of tensile properties of plain knitted fabric reinforced composites, Advanced Composite Materials, 6:2, 123-151

To link to this article: http://dx.doi.org/10.1163/156855197X00030

Adv. Composite Mater., Vol. 6, No. 2, pp. 123–151 (1997)

Analytical methods for prediction of tensile properties of plain knitted fabric reinforced composites

S. RAMAKRISHNA,[1] Z. MAEKAWA[2] and N. K. CUONG[2]

[1]*Department of Mechanical and Production Engineering, Faculty of Engineering, The National University of Singapore, 10 Kent Ridge Crescent, 119260 Singapore*
[2]*Department of Polymer Science and Engineering, Faculty of Textile Science, Kyoto Institute of Technology, Matsugasaki, Sakyo-ku, Kyoto 606, Japan*

Received December 15 1995; accepted May 31 1996

Abstract—This paper describes analytical models for predicting the elastic and tensile strength properties of knitted fabric reinforced composites. Owing to the looped yarn architecture, knitted fabric composites possess fiber and resin-rich regions. Initially, a geometric model has been identified for estimating the orientation of yarn in the knitted fabric. Using the unit cell approach, a 'cross-over model' has been proposed for expressing the cross-over of curved yarns of knitted fabric. Using laminated plate theory, the effective elastic properties of the yarns in the cross-over model have been estimated. Elastic properties of the composite were determined by combining the effective elastic properties of the curved yarns and the resin-rich regions. Tensile strength properties have been predicted by estimating the fracture strength of yarns bridging the fracture plane. Tensile properties of knitted fabric composites with different volume fraction of fibers were predicted. The analytical procedures have been validated by comparing one set of experimental results with the predictions. The applicability and limitation of these models have been discussed.

Keywords: knitted fabric composites; analytical model; cross-over model; elastic properties; tensile strength; fiber orientation; geometric model; fiber volume fraction.

1. INTRODUCTION

Recently, in the interest of reducing manufacturing cost, and enhancing processability and damage tolerance, knitted fabric reinforced composite materials have been receiving greater attention in the composite industry [1–3]. A number of experimental works on the mechanical properties of knitted fabric composites are now available in the literature [4–21]. However, only limited work has been reported on the modeling aspects of mechanical properties of knitted fabric composites.

Ko *et al.* [8] made initial efforts to predict the tensile properties of multidirectional warp knitted fabric reinforced composites using a unit cell concept and a modified laminate theory. The knitted fabric investigated is a special case, the unit cell of which contains five basic yarn components: 0° (weft), 90° (warp), 45° (bias), −45° (bias)

and the stitching yarn (throughthickness). In general in knitted fabrics, the yarns are curved and their orientation changes continuously along the loop. Hence, this model needs to be modified for predicting the tensile properties of other knitted fabric composites.

Rudd *et al.* [12] and Ramakrishna and Hull [16] made efforts to predict the elastic moduli of weft knitted fabric reinforced composites. They predicted elastic moduli using a combination of rule of mixtures and Krenchel's reinforcement efficiency factor. The agreement with the experimental results appeared to be good. They considered fiber orientation in the planar direction of the knitted fabric only. However, in the knitted fabric composite, the fibers are oriented three-dimensionally. Hence, a new approach is necessary to consider the three-dimensional orientation of fibers and also to predict tensile properties of composite material more accurately.

Primary objectives of this work are: 1) develop analytical functions for estimating the fiber orientation and fiber content of the composite and 2) develop analytical procedures for predicting the elastic and tensile strength properties of plain weft knitted fabric reinforced composites.

2. ANALYTICAL PROCEDURE FOR PREDICTION OF ELASTIC PROPERTIES

The research work described here is concerned mainly with a plain weft knitted fabric (Fig. 1). Owing to the looped yarn architecture, knitted fabric composites possess yarn and resin-rich regions. An outline of the analytical procedure for predicting the elastic properties of knitted fabric reinforced composite is shown in Fig. 2. Initially, a geometric model has been identified for estimating the orientation of yarn in the knit loop (Section 2.1). The main input parameters for this model are wale density (W), course density (C) and yarn diameter (d). Both C and W can be measured experimentally. W is defined as the number of wales per 2 cm length in the course direction of the fabric. Similarly, C is the number of courses per 2 cm length in the wale direction. The procedure for estimation of d is outlined in Section 2.2. Using the unit cell approach, a 'cross-over model' has been proposed for expressing the cross-over of curved yarns of knitted fabric. Using laminated plate theory, the effective elastic properties of the yarns were estimated (Section 2.4). The elastic properties of the composite were determined by combining the effective elastic properties of the yarns and resin-rich regions.

2.1. Geometric model

2.1.1. Determination of yarn orientation. A schematic diagram of an idealized unit cell of knitted fabric is shown in Fig. 3. The physical meaning of various symbols used are also shown in the figure. The basic assumptions are 1) yarns assume circular cross-section and 2) the projection of the central axis of the yarn on the plane of the fabric is composed of circular arcs, i.e. the yarn forming a course lies on the surface of a series of circular cylinders whose generators are perpendicular to the plane of the

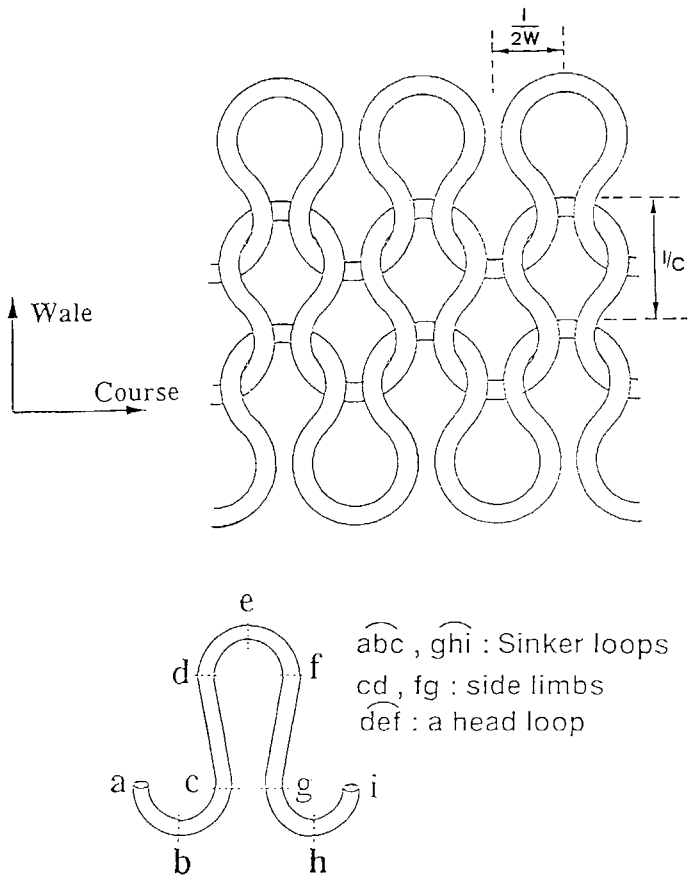

Figure 1. Schematic diagram of a plain weft knitted fabric.

fabric. These assumptions are reasonable as the knit loops are formed during knitting by bending the yarn round a series of equally spaced knitting needles and sinkers. The composite is made when the fabric is in relaxed condition without any pre-stretching. Due to the space constraint, only the required equations are presented in this paper. Detailed derivations of these equations may be found elsewhere [22, 23].

Consider rectangular axes Ox and Oy parallel to the wale and course directions of the fabric. The OQ portion of the loop is assumed to have center at C. The total angle of the portion of the loop under consideration, OCQ = φ. ad is the radius of projection of knit loop, CO, where a is a constant. Q is the point at which the central axis of this loop joints the central axis of the loop with center F. H and J are the points at which the yarns of adjacent loops (loops with centers at C and B) cross-over. The angles OCB = ψ and HCB = ϕ. If P is any point on the projection of the central axis, angle OCP = θ. The coordinates of point P are given by:

$$x = ad\,(1 - \cos\theta), \quad y = ad\sin\theta, \quad z = \frac{hd}{2}(1 - \cos\pi\theta/\varphi), \tag{1}$$

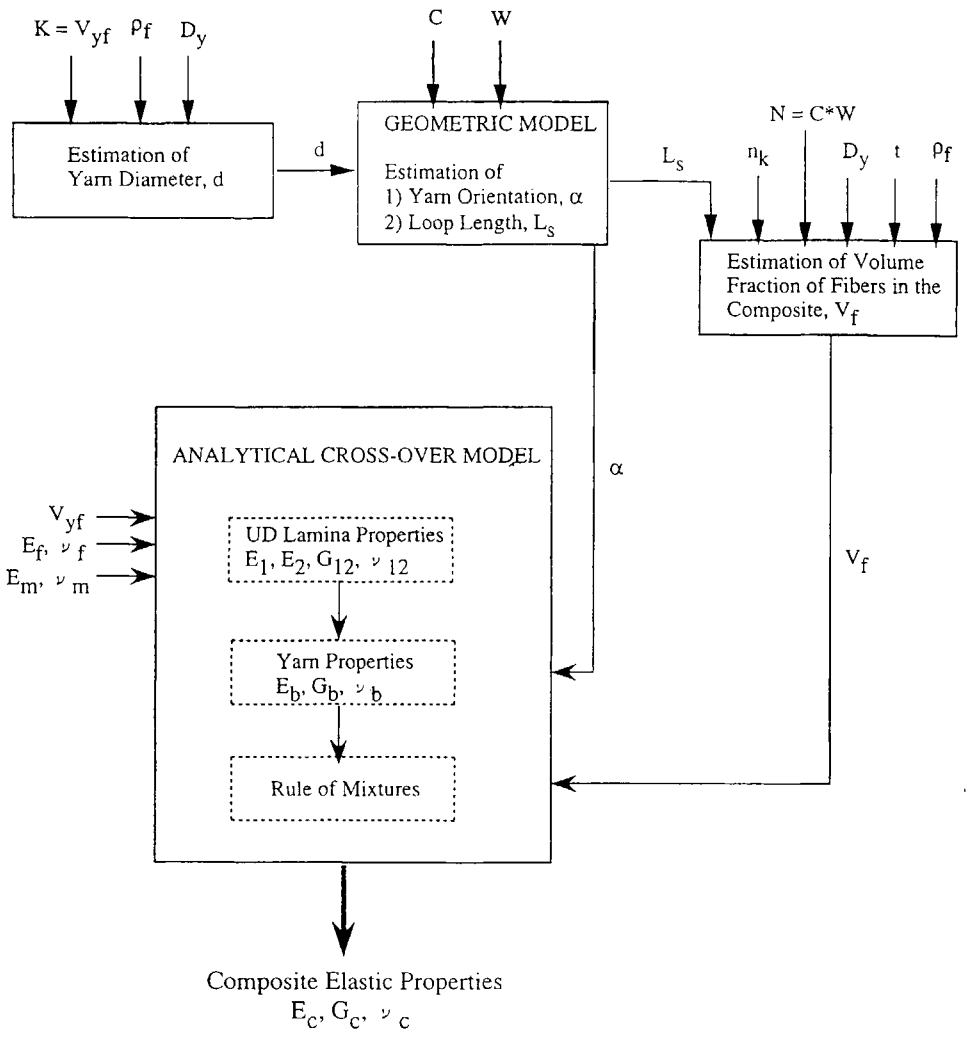

Figure 2. A flow chart of the analysis method for predicting the elastic properties of knitted fabric reinforced composite.

where h is a constant used for representing maximum height hd (at Q) of the central axis above the plane of the fabric. The unknown parameters in the equation (1) are a, h and φ. It is difficult to measure these parameters experimentally, but they may be determined from the simple geometric relations of the loop:

$$a = \frac{1}{4Wd\sin\varphi}, \tag{2}$$

$$\varphi = \pi + \sin^{-1}\left\{\frac{C^2 d}{[C^2 + W^2(1 - C^2d^2)^2]^{1/2}}\right\} - \tan^{-1}\left\{\frac{C}{W(1 - C^2d^2)}\right\}, \tag{3}$$

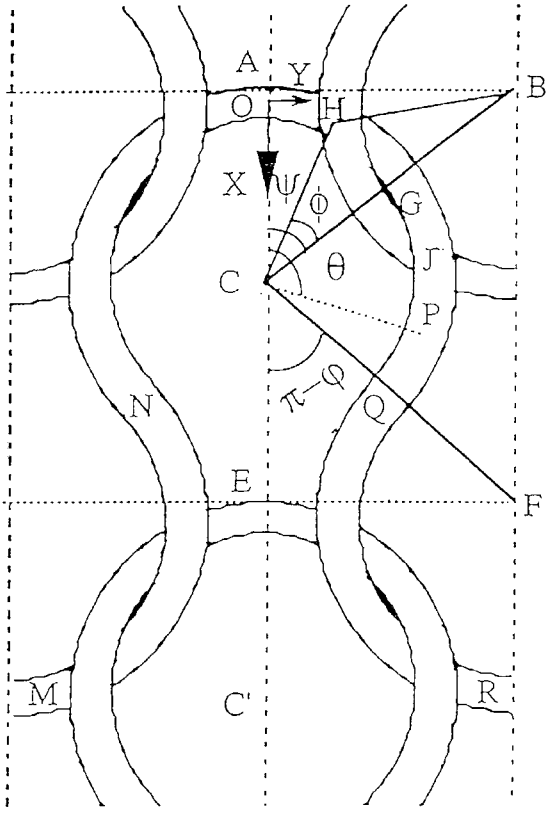

Figure 3. Schematic representation of a unit cell of knitted fabric.

$$h = \left[\sin\left(\frac{\pi\psi}{\varphi}\right) \sin\left(\frac{\pi\phi}{\varphi}\right) \right]^{-1}. \tag{4}$$

To determine h we need to know the angles ϕ and ψ, which are given by

$$\psi = \sin^{-1}\left(\frac{2a}{2a-1}\sin\varphi\right), \tag{5}$$

$$\phi = \cos^{-1}\left(\frac{2a-1}{2a}\right). \tag{6}$$

The orientation of yarn in a knit loop (MNOQR) can be determined by knowing the orientation of yarn in the portion OQ (Fig. 3). It can be assumed that the OQ portion of the loop is an assemblage of many small pieces of straight lines. Let us assume that $(x_{n-1},\ y_{n-1},\ z_{n-1})$ and $(x_n,\ y_n,\ z_n)$ are the coordinates of start and end points of each segment under consideration, respectively (Fig. 4). The length of each

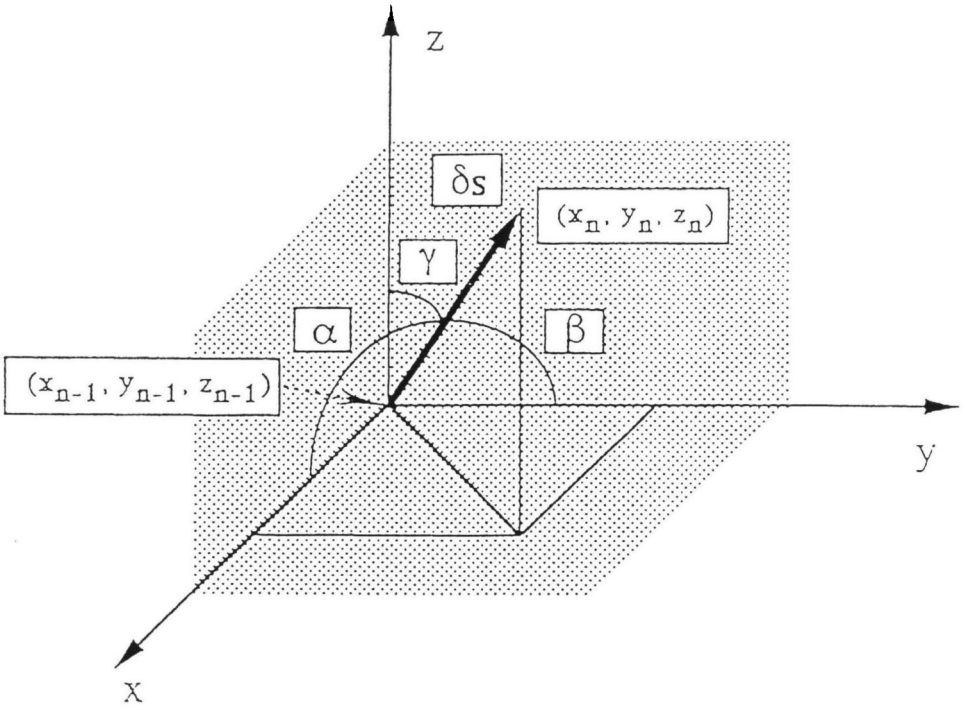

Figure 4. Representation of vector of a short segment of yarn.

segment, δs is given by

$$\delta s = \sqrt{([x_n - x_{n-1}]^2 + [y_n - y_{n-1}]^2 + [z_n - z_{n-1}]^2)}. \tag{7}$$

The orientations α, β and γ of segment with respect to the x, y and z axes, respectively are:

$$\alpha = \cos^{-1} \frac{x_n - x_{n-1}}{\delta s}, \quad \beta = \cos^{-1} \frac{y_n - y_{n-1}}{\delta s}, \quad \gamma = \cos^{-1} \frac{z_n - z_{n-1}}{\delta s}. \tag{8}$$

2.1.2. Determination of loop length. If L is the length of yarn from O to Q, it is given by

$$L \approx ad\varphi. \tag{9}$$

Considering the symmetry of the loop, the length of yarn in one loop (MNOQR) is given by

$$L_s \approx 4ad\varphi, \tag{10}$$

where L_s is the length of yarn in one loop.

2.2. Estimation of yarn diameter (d)

Hearle *et al.* [24] proposed two basic idealized packing models of circular fibers in yarns: open packing and close packing, in which the fibers are arranged in concentric and hexagonal patterns, respectively. The packing fraction of yarn (K) is defined as

$$K = \frac{A_f}{A_y}, \tag{11}$$

where A_y and A_f are the areas of yarn and fibers in the yarn, respectively. Typical values of K are 0.75 and 0.91 for open and closed packing patterns, respectively. However, experimental investigations indicate [14] that for weft knitted fabric reinforced composites $K = 0.45$, much smaller than the ideal packing conditions.

A_f is given by

$$A_f = \frac{D_y}{C_d \rho_f}, \tag{12}$$

where D_y is the linear density of the yarn, measured using the Denier count method (Denier is defined as the number of grams per 9000 meters of yarn); $C_d = 9 \times 10^5$, is a constant; ρ_f is the density of fiber (g/cm^3).

Combining equations (11) and (12) we get

$$A_y = \frac{D_y}{C_d \rho_f K}. \tag{13}$$

The yarn diameter, d, is given by

$$d = \sqrt{\frac{4D_y}{\pi C_d \rho_f K}}. \tag{14}$$

2.3. Estimation of fiber volume fractions

Due to the large resin-rich regions in the knitted fabric composite, it is reasonable to assume that the volume fraction of fibers in the composite (V_f) is smaller than volume fraction of fibers in the impregnated yarn (V_{yf}). Assuming the yarn is uniform along the length, the volume fraction of fibers in the impregnated yarn (V_{yf}) is given by

$$V_{yf} = K. \tag{15}$$

The volume fraction of fibers in the composite, V_f is given by

$$V_f = \frac{n_k D_y L_s C W}{C_d \rho_f A t}, \tag{16}$$

where L_s is the length of yarn in one loop or stitch and given by equation (10); t is the thickness of composite specimen; n_k is the number of layers of knitted fabric

in the composite; A is the planar area of the composite over which W and C are measured. In the present work, both C and W are measured over a unit length of 2 cm and hence $A = 4\ \text{cm}^2$.

Knitted fabrics are often specified using stitch density, N. N is defined as the number of knit loops per unit planar area of the fabric. The product of C and W gives N, and hence the equation (16) can be rewritten as

$$V_f = \frac{n_k D_y L_s N}{C_d \rho_f A t}. \tag{17}$$

2.4. *Estimation of elastic properties*

The unit cell of plain knitted can be divided into four identical sub-structures shown in Fig. 5(a). Each sub-structure consists of two impregnated yarns that cross-over each other. This sub-structure is called the 'cross-over model'. A three-dimensional representation of the cross-over model is shown in Fig. 5(b). Using the cross-over model, an unit cell can be constructed. Repeating the unit cell in the fabric plane obviously reproduces the complete plain knitted fabric structure. Hence, analysis of the cross-over model was carried out. In the modeling process, each impregnated yarn is further idealized as a curved unidirectional lamina. The elastic properties of a unidirectional lamina are given by [25]

$$\begin{aligned}
E_1 &= E_f V_{yf} + E_m(1 - V_{yf}),\\
\frac{1}{E_2} &= \frac{1.36\left(\frac{E_f}{1-\nu_f^2} - \frac{E_m}{1-\nu_m^2}\right)}{\left(\frac{E_f}{1-\nu_f^2} - \frac{E_m}{1-\nu_m^2}\right)^2 - \left(\frac{\nu_f E_f}{1-\nu_f^2} - \frac{\nu_m E_m}{1-\nu_m^2}\right)^2} + \frac{1 - 1.05\sqrt{V_{yf}}}{E_m},\\
\frac{1}{G_{12}} &= \frac{1.36}{\frac{E_f}{2(1+\nu_f)} - \frac{E_m}{2(1+\nu_m)}} + \frac{1 - 1.05\sqrt{V_{yf}}}{\frac{E_m}{2(1+\nu_m)}},\\
\nu_{12} &= \frac{1.05\sqrt{V_{yf}}(\nu_f - \nu_m)\left(\frac{E_f}{1-\nu_f^2}\right)}{\left(\frac{E_f}{1-\nu_f^2} - \frac{E_m}{1-\nu_m^2}\right)} + \nu_m,
\end{aligned} \tag{18}$$

where E_1, E_2, G_{12} and ν_{12} represent the longitudinal elastic modulus, transverse elastic modulus, in-plane shear modulus and Poisson ratio, respectively; E_f, ν_f and E_m, ν_m are the elastic moduli and Poisson ratios of fiber and resin matrix, respectively. Material constants of glass fiber epoxy resin are given in Table 1.

Assuming that the yarn is an assemblage of short segments, the orientation of each segment is given by equation (8).

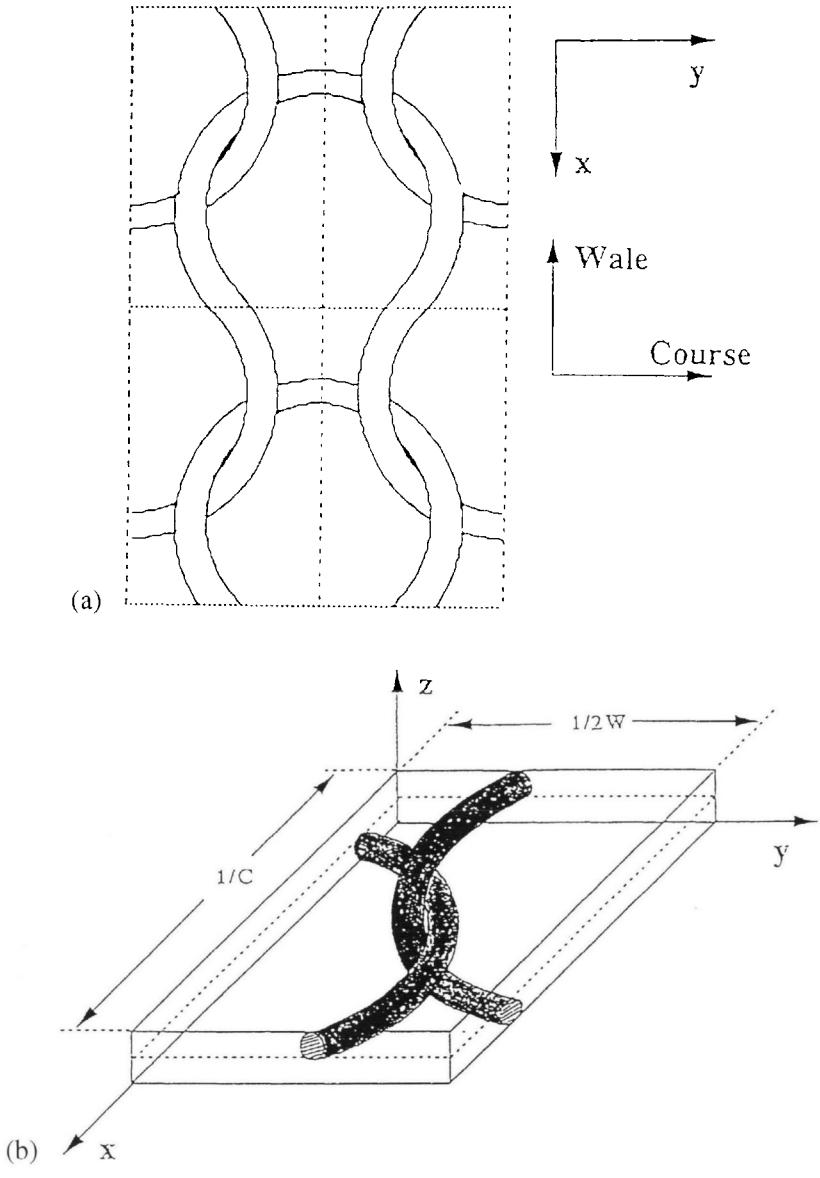

Figure 5. Schematic diagrams (a) unit cell and (b) cross-over model.

Table 1.
Material constants of glass fiber and neat epoxy resin

	Elastic modulus, GPa	Poisson ratio
Glass fiber	74	0.23
Epoxy resin	3.6	0.35

The reduced lamina effective elastic properties of each small piece in the x direction can be derived as follows [26, 27]:

$$E_x(\alpha) = \left[\frac{\cos^4\alpha}{E_1} + \left(\frac{1}{G_{12}} - \frac{2\nu_{12}}{E_1}\right)\sin^2\alpha\cos^2\alpha + \frac{\sin^4\alpha}{E_2}\right]^{-1},$$

$$E_y(\alpha) = \left[\frac{\sin^4\alpha}{E_1} + \left(\frac{1}{G_{12}} - \frac{2\nu_{12}}{E_1}\right)\sin^2\alpha\cos^2\alpha + \frac{\cos^4\alpha}{E_2}\right]^{-1},$$

$$\nu_{xy}(\alpha) = E_x(\alpha)\left[\frac{\nu_{12}}{E_1}\left(\sin^4\alpha + \cos^4\alpha\right) - \left(\frac{1}{E_1} + \frac{1}{E_2} - \frac{1}{G_{12}}\right)\sin^2\alpha\cos^2\alpha\right], \quad (19)$$

$$G_{xy}(\alpha) = \left[2\left(\frac{2}{E_1} + \frac{2}{E_2} + \frac{4\nu_{12}}{E_1} - \frac{1}{G_{12}}\right)\sin^2\alpha\cos^2\alpha + \frac{1}{G_{12}}\left(\sin^4\alpha + \cos^4\alpha\right)\right]^{-1},$$

where $E_x(\alpha)$ and $E_y(\alpha)$ are the elastic moduli of the segment in the x and y directions, respectively; $G_{xy}(\alpha)$ and $\nu_{xy}(\alpha)$ represent shear modulus and Poisson ratio of the segment, respectively.

In the composite from, these segments may be subjected to different stresses and strains depending on their orientation, relative distribution with respect to each other, and the material properties of the reinforcement fibers and resin. During tensile testing, in the elastic region, no debonding between the yarns and matrix resin was observed. In other words, both the yarn and resin were being stretched equally and hence, we assume that the composite was subjected to a uniform strain condition. It is to be noted that this is one of the many possible assumptions and this assumption is a limitation of the proposed method for estimating elastic properties of knitted fabric composites.

Assuming that all the segments are subjected to same strain condition:

$$\overline{E}_x = \frac{1}{L}\int_0^L E_x(\alpha)\mathrm{d}x, \quad \overline{E}_y = \frac{1}{L}\int_0^L E_y(\alpha)\mathrm{d}x, \quad \overline{G}_{xy} = \frac{1}{L}\int_0^L G_{xy}(\alpha)\mathrm{d}x,$$

$$\overline{\nu}_{xy} = \frac{1}{L}\int_0^L \nu_{xy}(\alpha)\mathrm{d}x, \quad \overline{\nu}_{yx} = \overline{\nu}_{xy}\frac{\overline{E}_y}{\overline{E}_x}, \quad (20)$$

where L is given by equation (9).

The stiffness matrix of curved yarn is [26]

$$\overline{\mathbf{Q}}_{ij} = \begin{bmatrix} \dfrac{\overline{E}_x}{(1-\overline{\nu}_{xy}\overline{\nu}_{yx})} & \dfrac{\overline{\nu}_{yx}\overline{E}_x}{(1-\overline{\nu}_{xy}\overline{\nu}_{yx})} & 0 \\ \dfrac{\overline{\nu}_{yx}\overline{E}_x}{(1-\overline{\nu}_{xy}\overline{\nu}_{yx})} & \dfrac{\overline{E}_y}{(1-\overline{\nu}_{xy}\overline{\nu}_{yx})} & 0 \\ 0 & 0 & \overline{G}_{xy} \end{bmatrix}. \tag{21}$$

The above equations have been developed for one curved yarn. The cross-over model consists of two curved yarns. From the geometry of knit loops, the orientation of the second yarn can be obtained by rotating the first yarn by 180° in a clockwise direction. Using $\alpha = (\alpha + \pi)$ and equations (19), (20) and (21), the effective elastic properties of the second yarn can be obtained.

The stiffness constants of both the yarns of the cross-over model are known. The elastic properties of the cross-over model can be derived assuming that each of the curved yarns is subjected to the same strain along the x direction. The total effective stiffness parameters of both the yarns of cross-over model are given by [26]

$$\mathbf{A}_{ij} = \sum_{n=1}^{2} L_n \overline{\mathbf{Q}}_{ij}(n) \quad (i, j = 1, 2, S), \tag{22}$$

where n represents the yarn number.

Thus, the stiffness matrix of the yarns in the cross-over model is

$$\mathbf{A}_{ij} = \begin{bmatrix} A_{11} & A_{12} & 0 \\ A_{12} & A_{22} & 0 \\ 0 & 0 & A_{SS} \end{bmatrix}. \tag{23}$$

The effective elastic properties of the cross-over yarns are given by [26]

$$E_b = \frac{A_{11}A_{22} - A_{12}^2}{(L_1 + L_2)A_{22}}, \quad \nu_b = \frac{A_{12}}{A_{22}}, \quad G_b = \frac{A_{SS}}{(L_1 + L_2)}, \tag{24}$$

where L_1 and L_2 are the lengths of yarns in the cross-over model; E_b, G_b and ν_b are the combined elastic modulus, in-plane shear modulus and Poisson ratio of both yarns in the cross-over model, respectively.

Equation (24) gives the combined elastic properties of the yarns only. The elastic properties of the composite can be determined by combining the elastic properties of the yarns and resin-rich regions. For this purpose we need to know the relative volume fractions of yarns and the resin-rich regions in the composite.

The volume fraction of yarns in the composite, V_b, can be determined as follows. V_{yf} is the ratio of volume of fibers to volume of impregnated yarns. Similarly, v_f is

the ratio of volume of fibers to volume of composite. Hence, the volume fraction of impregnated yarns in the composite is given by

$$V_b = V_f / V_{yf}, \tag{25}$$

where V_{yf} and V_f are given equations (15) and (16), respectively.

The effective elastic modulus of the composite is given by the rule of mixtures,

$$E_c = (E_b)(V_b) + (E_m)(1 - V_b). \tag{26}$$

Similarly, shear modulus G_c and Poisson's ratio ν_c of the composite are given by [25]

$$G_c = \left[\frac{1.36}{\frac{E_b}{2(1+\nu_b)} - \frac{E_m}{2(1+\nu_m)}} + \frac{1 - 1.05\sqrt{V_b}}{\frac{E_m}{2(1+\nu_m)}} \right]^{-1}, \tag{27}$$

$$\nu_c = \frac{1.05\sqrt{V_b}(\nu_b - \nu_m)\left(\frac{E_b}{1-\nu_b^2}\right)}{\left(\frac{E_b}{1-\nu_b^2} - \frac{E_m}{1-\nu_m^2}\right)} + \nu_m. \tag{28}$$

3. ANALYTICAL PROCEDURE FOR ESTIMATING TENSILE STRENGTH

Assuming that the ultimate fracture of the composite occurs due to the simultaneous fracture of matrix and reinforcement fibers, the tensile strength of knitted fabric reinforced composite (σ_c) can be estimated using the rule of mixtures

$$\sigma_c = (V_f)(\sigma_f)\cos^2\overline{\alpha} + (\sigma_m)(1 - V_f), \tag{29}$$

where σ_f and σ_m are the tensile strengths of reinforcement fibers and matrix resin, respectively; $\overline{\alpha}$ is the average orientation of yarn with respect to the loading direction.

However, Ramakrishna and Hull [15] showed experimentally that the failure strength of knitted fabric reinforced epoxy composites depends mainly on the yarn bundles bridging the fracture plane (Fig. 6). The number of yarns bridging the fracture plane would depend on the testing direction with respect to the knitted fabric. The present study is concerned with the wale direction properties. The wale tensile strength of knitted fabric composite is dependent on the number of yarn bundles (n_b) bridging the wale fracture plane:

$$n_b = n_k(2)\frac{W}{2}B, \tag{30}$$

where B is the width of tensile specimen in cm.

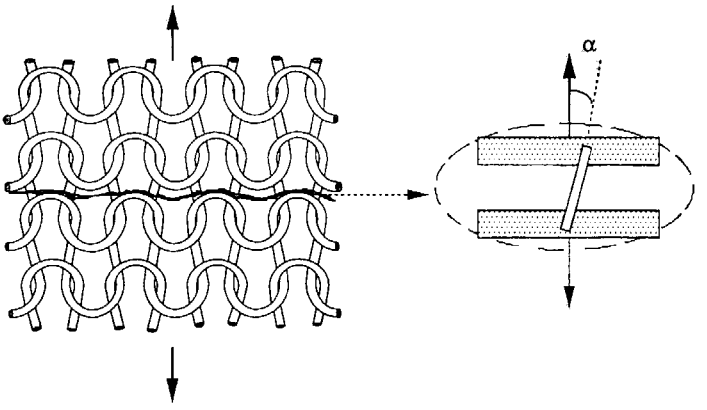

Figure 6. Schematic diagrams illustrating wale fracture plane and a yarn bundle bridging the fracture plane.

The area fraction of yarn bundles (A_b) bridging the fracture plane is given by

$$A_b = \frac{n_k(2)\frac{W}{2}B\frac{\pi d^2}{4}}{Bt},$$

$$A_b = \frac{n_k W \pi d^2}{4t}, \tag{31}$$

where t is the specimen thickness in cm; d is the yarn diameter given by equation (14).

The strength of knitted fabric composite (σ_c) in the wale direction is given by

$$\sigma_c = (A_b)(\overline{\sigma_b}),$$

$$\sigma_c = \frac{n_k W \pi d^2[\overline{\sigma_b}]}{4t}, \tag{32}$$

where $\overline{\sigma_b}$ is the mean strength of the set of yarn bundles bridging the fracture plane. The $\overline{\sigma_b}$ can be estimated using the following procedure. Assuming that all the bridging yarns possess the same tensile strength and are aligned perfectly in the loading direction, the $\overline{\sigma_b}$ will be equal to the longitudinal tensile strength of a unidirectional lamina (σ_1):

$$\overline{\sigma_b} = \sigma_1 = (\sigma_f)(V_{yf}) + (\sigma_m)(1 - V_{yf}). \tag{33}$$

However, owing to their looped architecture, it is reasonable to assume that the yarns in the fracture plane orient at an angle α with respect to the loading direction (Fig. 6). An approximate estimate of α can be obtained using equation (8). The yarn bundle can be treated as an off-axis loaded unidirectional lamina. Hence, the tensile strength

of a yarn bundle is given by [27]

$$\sigma_b = \left[\frac{\cos^4 \alpha}{\sigma_1^2} + \frac{\sin^4 \alpha}{\sigma_2^2} + \frac{\sin^2 \alpha \cos^2 \alpha}{\tau_{12}^2} - \frac{\sin^2 \alpha \cos^2 \alpha}{\sigma_1^2} \right]^{-1/2}, \tag{34}$$

where σ_1, σ_2 and τ_{12} are the longitudinal, transverse and shear strengths of unidirectional lamina, respectively (Table 2).

Typical variation of σ_b with α is shown in Fig. 7: σ_b decreased with increasing α. The decrease of σ_b was significant in the range $0° < \alpha < 15°$. Hence, the effect of the variation of σ_b with α in this range on the composite strength was analyzed. All the yarn bundles in the fracture plane may not have same α value, since the fracture path is irregular and occurs at different positions of the knit loops. During tensile testing the yarn bundles are peeled (debonded) from the fracture surface and stretched before their failure. Due to the peeling and stretching effect, the yarn bundles try to align in the testing direction. Determination of actual α just before the failure of yarn bundle is a difficult task. It may be the case that different yarn bundles orient at different α with respect to the loading direction. It can be expected that yarn bundles bridging the fracture plane possess different strength values arising from different values of α. The yarn bundles may also possess different strengths due to the statistical distribution of the fiber strength. Many researchers have investigated the statistical nature of bundle strengths. The present study is concerned mainly with the variation of σ_b with α. From Fig. 7, an exponential relationship between σ_b and α is given by

$$\sigma_b = Pe^{-Q\alpha}, \tag{35}$$

where P and Q are parameters of exponential function and can be determined using the following equations (36) and (37), respectively.

When $\alpha = 0$,

$$P = \sigma_1. \tag{36}$$

If we assume that all the yarn bundles are oriented in the range $0 < \alpha < \alpha_k$, the maximum orientation, α_k, can be determined from the fracture surfaces. Let σ_{bk} be the bundle strength corresponding to the maximum orientation, α_k. From equations (35) and (36),

$$\sigma_{bk} = \sigma_1 e^{-Q\alpha_k}.$$

Table 2.
Tensile properties of unidirectional glass fiber/epoxy lamina

Longitudinal strength, σ_1 MPa	Transverse strength, σ_2 MPa	Shear strength, τ_{12} MPa
885	45	35

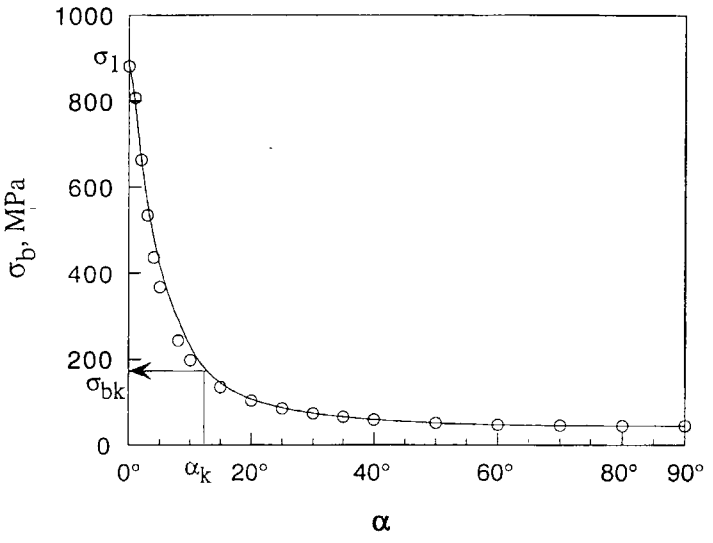

Figure 7. Typical variation of σ_b with α.

Rearranging this equation gives

$$Q = \frac{1}{\alpha_k} \ln\left(\frac{\sigma_1}{\sigma_{bk}}\right). \tag{37}$$

Equation (35) indicates the changes in σ_b with α. Equation (30) gives the number of yarn bundles bridging the fracture plane. It is necessary to know how many of these bundles orient at each value of α. The following exponential function $f(\alpha)$ was assumed for expressing the orientation distribution of yarn bundles in the fracture plane:

$$f(\alpha) = Re^{-S\alpha}, \tag{38}$$

where R and S are the parameters of the exponential function.

This function suggests that more yarns orient close to the testing direction. This assumption is reasonable as the yarn bundles try to align in the loading direction due to the debonding and stretching mechanisms. Typical curves for the function $f(\alpha)$ are shown in Fig. 8. The area under a curve is unity; therefore

$$\int_0^{\alpha_k} f(\alpha)\mathrm{d}\alpha = \int_0^{\alpha_k} Re^{-S\alpha}\mathrm{d}\alpha = -\frac{R}{S}\left[e^{-S\alpha_k} - 1\right] = 1,$$

$$R = \frac{S}{\left[1 - e^{-S\alpha_k}\right]}. \tag{39}$$

R is dependent on the value of S and α_k. Typical $f(\alpha)$ curves for different S and α_k are shown in Fig. 8. These curves indicate that $f(\alpha)$ is more sensitive to the

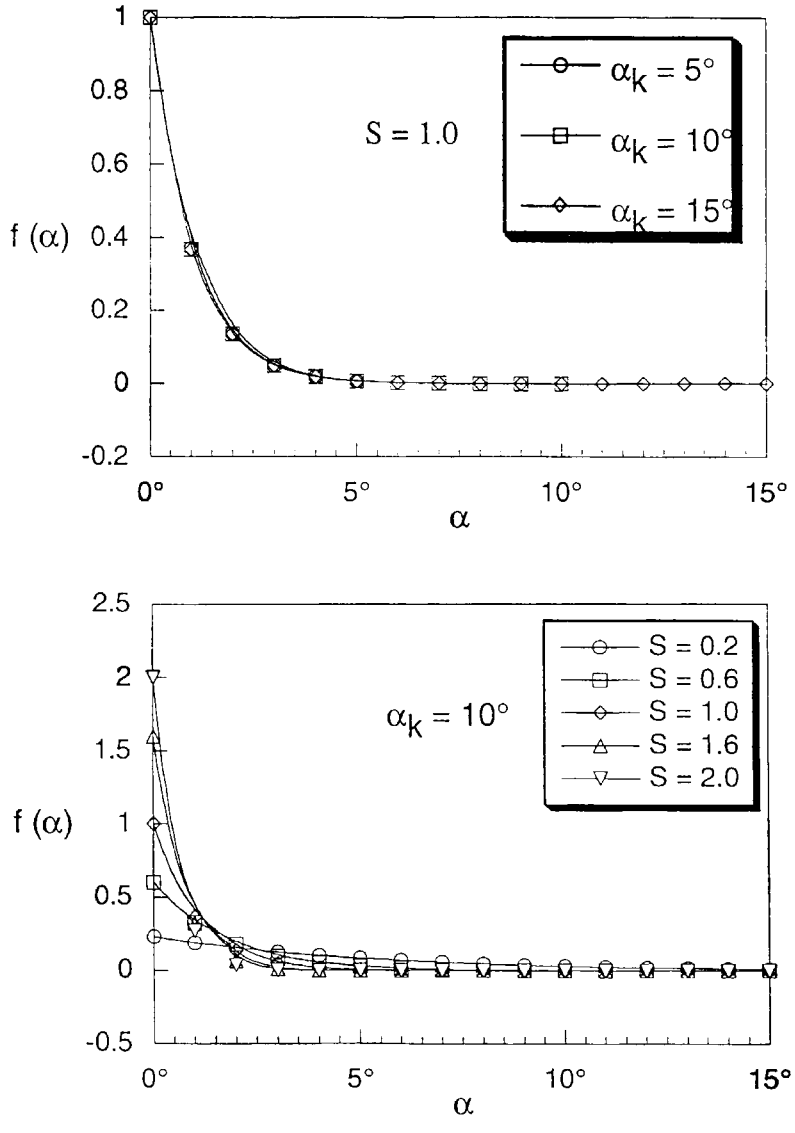

Figure 8. Typical curves of function $f(\alpha)$.

parameter S than α_k. When S is small, the yarn orientation distribution is spread out. For large values of S, the distribution is skewed and more yarns are aligned close to the loading direction.

Let $g(\sigma_b)$ be the function of yarn bundle distribution with respect to the bundle strength. Typical $g(\sigma_b)$ curves are shown in Fig. 9. Using the variable transformation technique,

$$g(\sigma_b)d\sigma_b = f(\alpha)d\alpha.$$

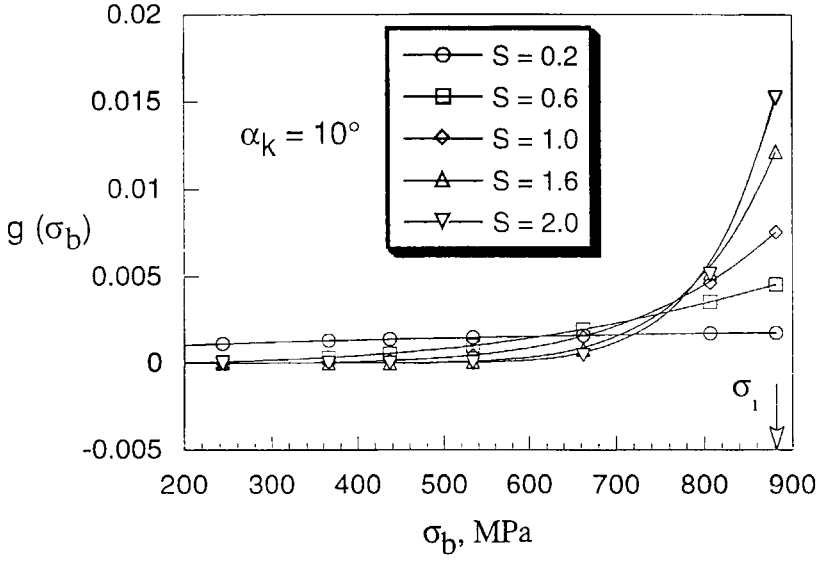

Figure 9. Typical curves of function $g(\sigma_b)$.

Rearranging this equation gives

$$g(\sigma_b) = f(\alpha)\left|\frac{d\alpha}{d\sigma_b}\right|. \tag{40}$$

From equations (35) and (40):

$$g(\sigma_b) = \frac{R}{PQ}e^{(Q-S\alpha)}. \tag{41}$$

From equation (35):

$$\alpha = \frac{-1}{Q}\ln\left(\frac{\sigma_b}{P}\right). \tag{42}$$

Combining equations (41) and (42):

$$g(\sigma_b) = \frac{R}{QP^{S/Q}}\sigma^{(S/Q-1)}. \tag{43}$$

Let $G(\sigma_b)$ indicate the yarn bundles fractured due to the applied stress, σ_b. The surviving yarn bundles $[1 - G(\sigma_b)]$ are given by

$$\left[1 - G(\sigma_b)\right] = \int_{\sigma_b}^{\sigma_1} g(\sigma_b)d\sigma_b,$$

$$\left[1 - G(\sigma_b)\right] = \frac{R}{SP^{S/Q}}\left[\sigma_1^{S/Q} - \sigma_b^{S/Q}\right]. \tag{44}$$

Let σ_{bm} be the value of bundle stress σ_b which gives $\sigma_b[1 - G(\sigma_b)]$ its maximum value, namely

$$\frac{d}{d\sigma_b}\left\{\sigma_b[1 - G(\sigma_b)]\right\}_{\sigma_b=\sigma_{bm}} = 0. \tag{45}$$

Equation (45) implies that the maximum yarn bundle stress, σ_{bm}, is found from the condition that at failure the load borne by the bundles is the maximum. Hence,

$$\sigma_{bm} = P\left[\frac{1}{1 + S/Q}\right]^{Q/S}. \tag{46}$$

The maximum mean strength ($\overline{\sigma_b}$) of surviving yarn bundles can be obtained by substituting the value of σ_{bm} in $\sigma_b[1 - G(\sigma_b)]$,

$$\overline{\sigma_b} = \frac{RP}{Q}\left[\frac{1}{1 + S/Q}\right]^{Q/S+1}. \tag{47}$$

For a given composite system, the parameter P is constant (equation (36)). Q is mainly dependent on the α_k and σ_{bk} (equation (37)). Parameter R is dependent on S and α_k (equation (39)). In other words, $\overline{\sigma_b}$ depends mainly on S and α_k. Typical variation of $\overline{\sigma_b}$ with S and α_k is shown in Fig. 10. Figure 10 clearly indicates that $\overline{\sigma_b}$ is mainly influenced by the parameter S. The $\overline{\sigma_b}$ initially increased rapidly with increasing S from 0.2 to 2.5, above which it increase only marginally. This behavior is expected, since large S means more yarns aligned close to the loading direction and hence higher mean bundle strength. Small values of S indicate that yarn orientation distribution is spread out and hence, lower mean bundle strength.

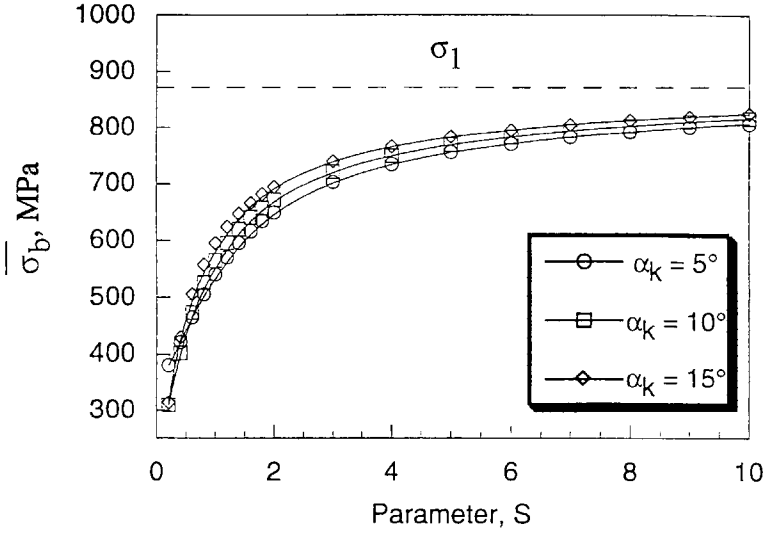

Figure 10. Typical variation of $\overline{\sigma_b}$ with parameters S and α_k.

Substituting equation (47) in equation (32), the knitted fabric composite tensile strength is given by

$$\sigma_c = \left\{\frac{n_k W \pi d^2}{4t}\right\}\left\{\frac{RP}{Q}\left[\frac{1}{1+S/Q}\right]^{Q/S+1}\right\}. \tag{48}$$

4. EXPERIMENTAL DETAILS

To check the validity of analytical methods outlined in this paper, a plain weft knitted fabric reinforced epoxy composite was fabricated. The plain knitted fabrics were produced on a flat bed weft knitting machine using glass fiber yarn (ECD 450 1/2 4-45Y-23, Nippon Electric Glass Co., Japan). The linear density of glass fiber yarn, $D_y = 1600$ Denier. The knitted fabric has $W = 4$ loops/2 cm and $C = 5$ loops/2 cm.

A single layer knitted fabric reinforced composite was made by the hand lay-up method using a mixture of epoxy resin (Epikote 828) and hardener, triethylenetetramine (11% of weight of epoxy resin). The composite was cured at 100°C for 1 h. The volume fraction of fibers (V_f) of the composite was 9.5%, estimated by combustion method. Composite specimens of 200 mm length, 20 mm width and 0.6 mm thickness were prepared by cutting parallel to the wale direction of the knitted fabric. Glass/epoxy end tabs of 50 mm length were glued to both ends of each specimen. Tensile tests were carried out using an Instron testing machine (Type 4206) at a cross-head speed of 1 mm/min. Strains were measured using a bi-axial strain gauge.

5. RESULTS AND DISCUSSION

5.1. Variation of tensile properties with fiber content

Tensile properties of composite materials are dependent on the volume fraction of fibers. Hence, initially, efforts have been made to estimate the volume fraction of fibers of the knitted fabric composite theoretically (Figs 11 to 13).

Figure 11 shows the variation of volume fraction of fibers (V_f) with the changes in the linear density of yarn (D_y). For a given stitch density of knitted fabric (N), the V_f increased linearly with increasing D_y. This behavior can be expected from the relationship between V_f and D_y described in equation (17). All the parameters in the denominator of equation (17) are constant. L_S is dependent on the N and yarn diameter, d. Assuming that N is constant, L_S depends mainly on d, which is proportional to D_y (equation (14)). Hence, from equation (17), the V_f is proportional to D_y. In other words, the fiber content of knitted fabric composites can be increased with increasing D_y. However, the maximum V_f that can be achieved is limited by the knitting needles used in the knitting machine. Increasing D_y means using coarser yarns. In general, the coarser yarns are difficult to knit and the coarsest yarn that can be used is dependent on the yarn type, knitting needle size and other devices used on

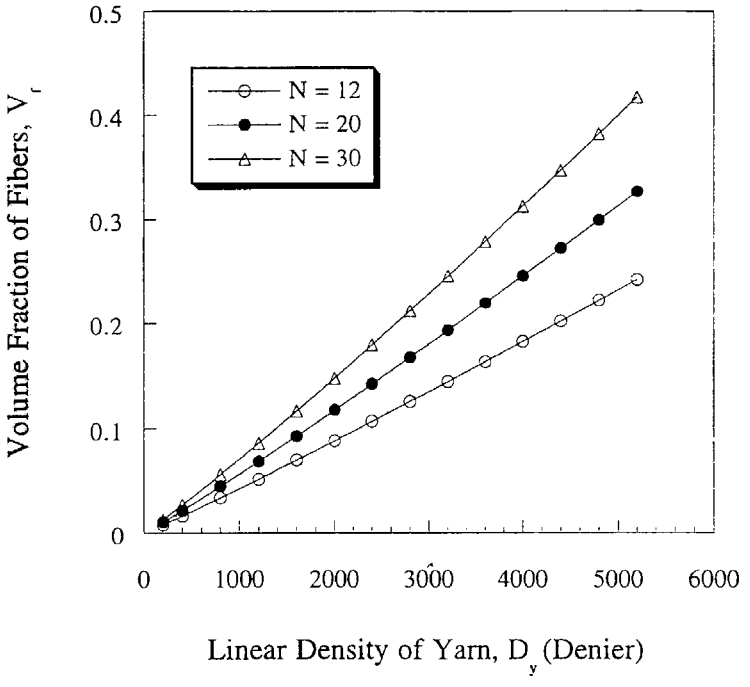

Figure 11. Variation of fiber volume fraction of composite with linear density of the yarn.

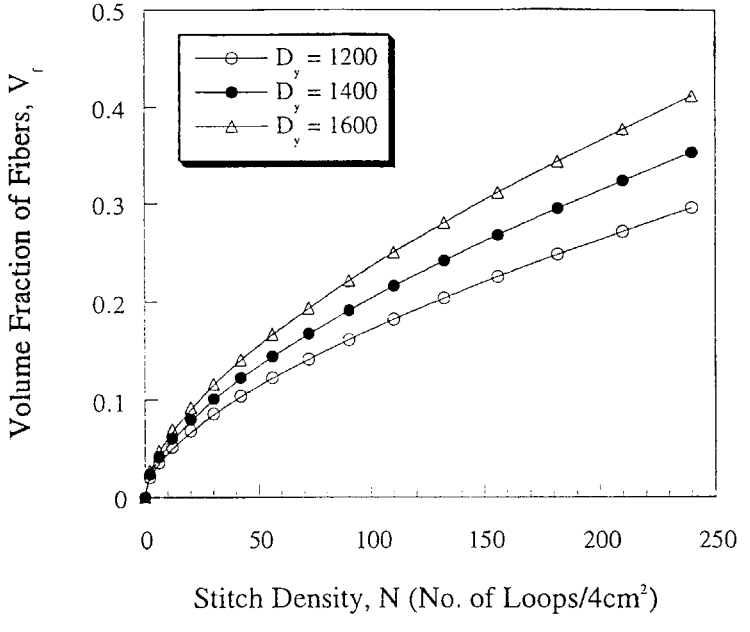

Figure 12. Variation of fiber volume fraction of composite with stitch density of knitted fabric.

the knitting machine. By assuming that it is possible to use yarns of different sizes, the variation of V_f with D_y is computed theoretically. These plots give an estimate of V_f that can be expected when different sizes of yarns are used.

For a constant D_y, the variation of V_f with N is shown in Fig. 12. The N of knitted fabric can be changed in two ways: 1) machine gauge and 2) stitch tightness control setting on the knitting machine. Machine gauge is defined as the number of needles per unit length of needle bed in the knitting machine. Most machines are equipped with a stitch tightness control button, used to alter N within a given range. Figure 12 suggests that V_f increases non-linearly with increasing N. This can be understood by examining equation (17). D_y and other parameters in the denominator of equation (17) are assumed to be constant. Hence, V_f is proportional to the product of L_S and N. An increase of N means smaller knit loops, which implies that stitch length, L_S, decreases with increasing N. The inverse relationship between the N and L_S results in non-linear variation of V_f with increasing N. Nevertheless, it can be said that V_f can be increased with increasing N. The maximum V_f that can be achieved with increasing N is limited by the yarn diameter, d. With increasing stitch density the course spacing, $1/C$ and wale spacing, $1/W$ decrease. In other words, the side limbs of a knit loop come closer with increasing stitch density or tightness of knitted fabric. The spacing between the limbs of a loop is approximately $1/(2W)$ (Fig. 1). The minimum spacing of side limbs is limited by the yarn diameter. To be able to stitch a knitted fabric, the condition $(1/(2W) \geqslant d)$ must be satisfied. The plots in Fig. 12 give an approximate idea of different V_f that can be achieved by changing N.

The relation between V_f and number of plies of knitted fabric (n_k) is shown in Fig. 13. For given D_y and N, the V_f can be increased with increasing n_k. This linear relationship can be understood from equation (17). However, it is to be noted that

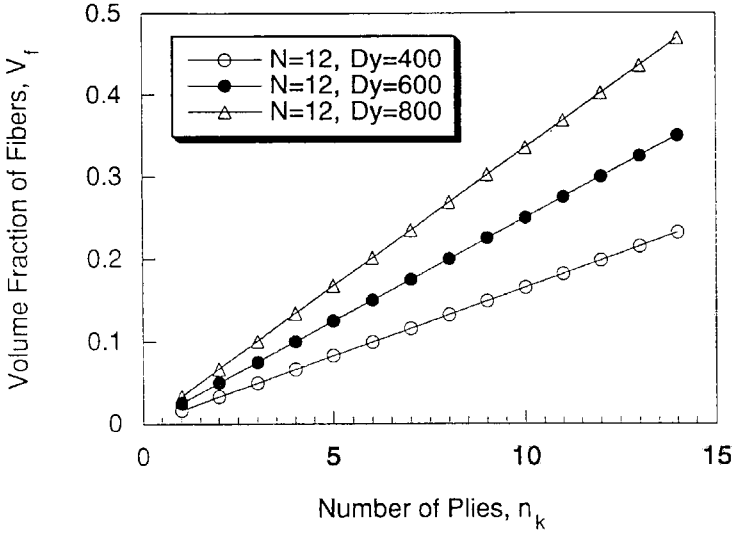

Figure 13. Variation of fiber volume fraction of composite with number of plies of knitted fabric.

the number of layers of knitted fabrics that can be used is limited by the thickness of the composite.

Figures 11 to 13 give an approximate idea of variation of V_f with D_y, N and n_k. The maximum V_f that can be achieved in knitted fabric composites is yet to be estimated, as it is dependent on many other parameters such as compressibility of knitted fabrics, composite fabrication conditions, etc. Efforts are being made to predict a theoretical maximum V_f that can be achieved in knitted fabric composites. Experimental research works reported in the literature suggest that a fiber volume fraction of 40% is realistically possible in knitted fabric composites. Hence, the tensile properties were predicted for fiber volume fractions less than 40%.

Using the analytical procedure outlined in Section 2 the elastic properties of knitted fabric composites were computed for different volume fraction of fibers. Figures 14, 15 and 16 show the variation of elastic properties of knitted fabric composites with the fiber content. In general, all the elastic properties increased linearly with increasing fiber content. For maximum $V_f = 41\%$, elastic modules, shear modules and Poisson ratio are 15.97 GPa, 2.56 GPa and 0.836, respectively. The elastic properties of knitted fabric composite are comparable to the continuous random fiber composite with similar fiber content [12].

Tensile strengths of knitted fabric composites of different V_f were computed using equation (48). The main assumptions are: 1) in the fiber content range investigated, the failure mechanisms of knitted fabric composites are similar and 2) the composite strength is determined mainly by the fracture strength of the yarns bridging the fracture plane. Figure 17 shows that the composite tensile strength varies with the parameters S and α_k. The composite strength is more sensitive to the parameter S than α_k. This behavior is similar to the variation of mean bundle strength, $\overline{\sigma}_b$ with S and α_k (Fig. 10). It is essential to determine the parameter S to obtain as accurate a prediction of composite strength as possible. In the present study, we experimentally investigated

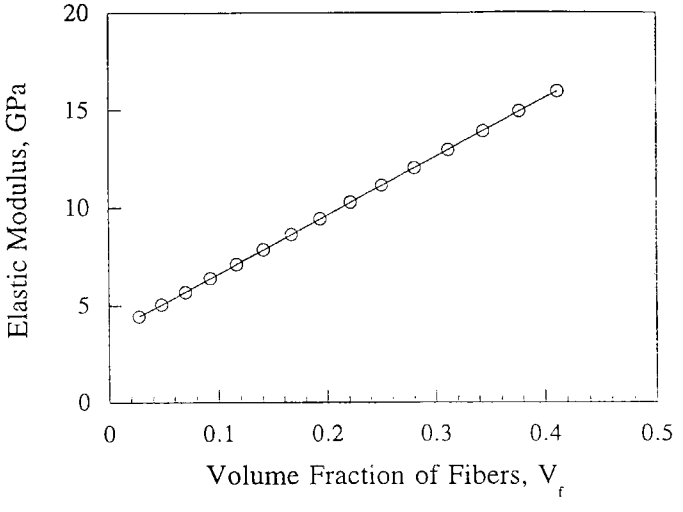

Figure 14. Variation of elastic modulus of knitted fabric composite with the fiber content.

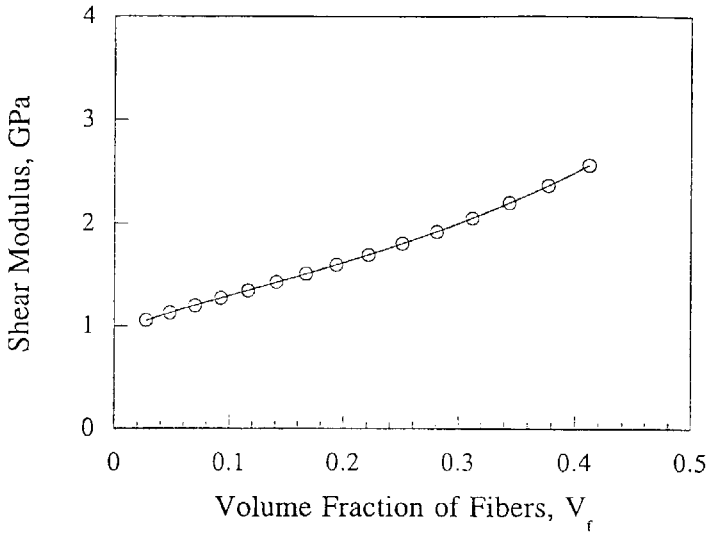

Figure 15. Variation of shear modulus of knitted fabric composite with the fiber content.

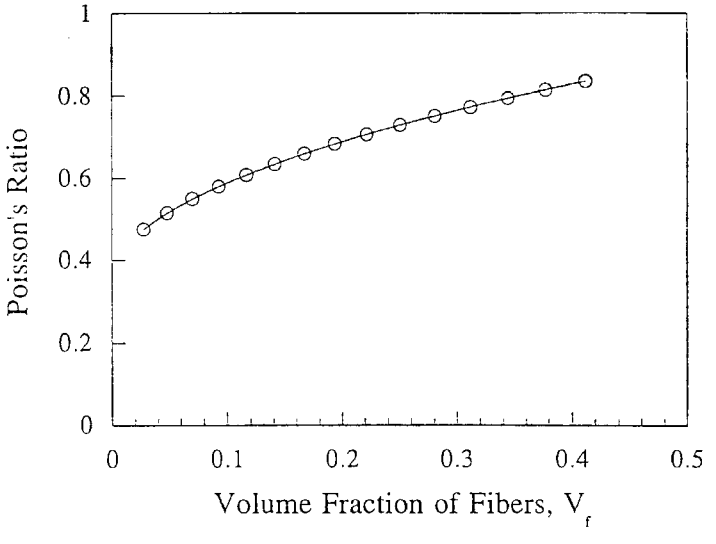

Figure 16. Variation of Poisson ratio of knitted fabric composite with the fiber content.

the tensile properties of knitted fabric composite with 9.5% volume fraction of fibers. Figure 17a, shows the comparison between the experimental strength and prediction curves. When $S = 1.25$, the predicted tensile strength matches the experimental result. Assuming that S is the same for all composites, tensile strengths of composites with different V_f were estimated. Composite tensile strength increased with increasing V_f. For $V_f = 9.25\%$, 18.5%, 27.8% and 37%, the estimated tensile strengths of knitted fabric composites were 65 MPa, 120 MPa, 175 MPa and 250 MPa, respectively.

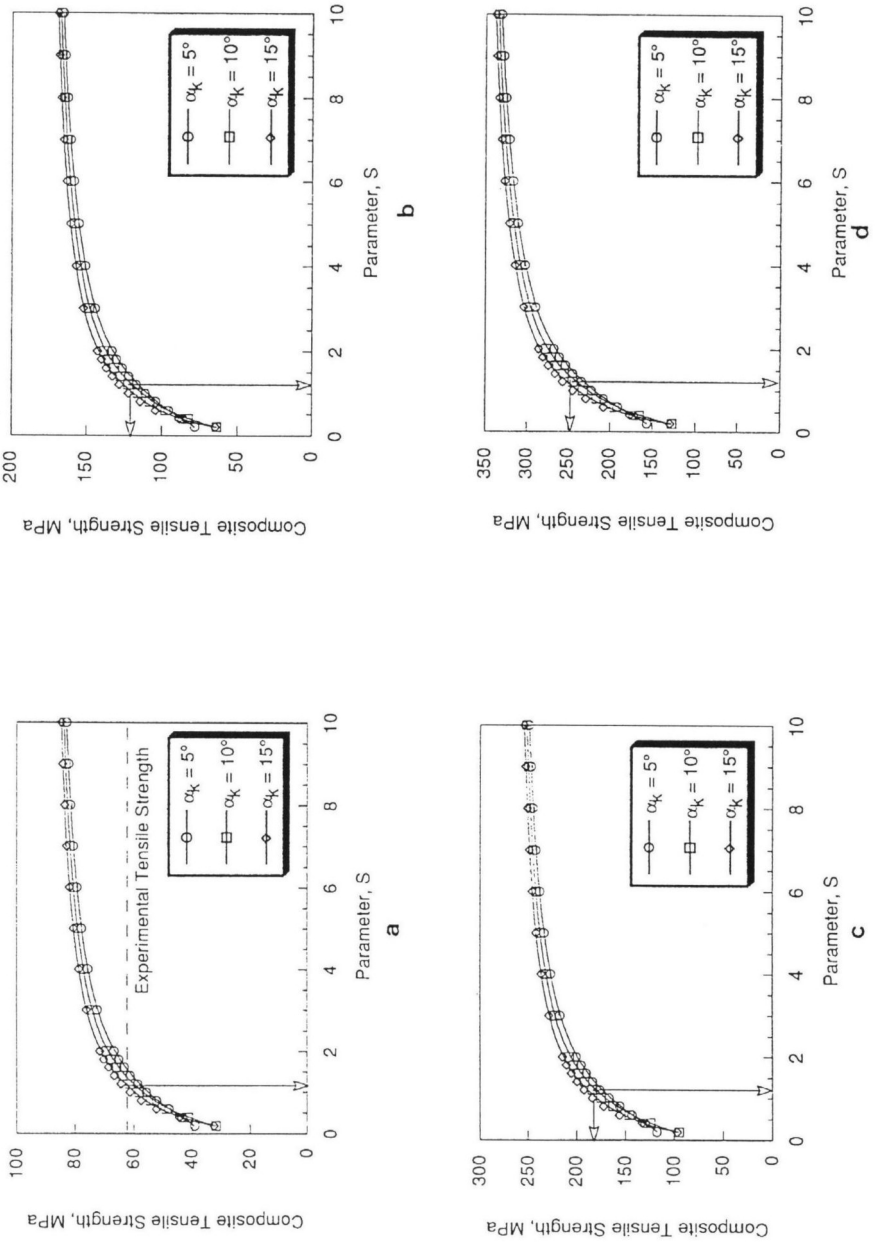

Figure 17. Tensile strengths of knitted fabric composite with fiber volume fractions a) 9.25%, b) 18.5%, c) 27.8% and d) 37%.

5.2. Comparison between analytical and experimental results

The typical stress–strain curve obtained from the tensile testing of glass fiber knitted fabric reinforced epoxy composite is shown in Fig. 18. Stress increased linearly with increasing strain up to knee point. The knee point occurred approximately at 0.45% strain. The non-linearity of the stress–strain curve above the knee point was associated with material deformation and microfracture processes in the specimen. Optical photographs of specimen taken at different stages of tensile testing are shown in Fig. 19. Initially, debonding of knit loop fiber bundles and micro-cracking of resin matrix occurred. With further increase of applied stress, the cracks grew through the resin rich regions in the widthwise direction of the specimen. The yarns bridging the fracture plane were observed. Peeling (debonding) of yarns from the fracture surfaces was also observed. The fracture of bridging yarns resulted in complete separation of fracture surfaces. Fracture surfaces indicate that $\alpha_k \approx 15°$. Elastic modulus was calculated from the initial linear portion of the stress–strain curve. Tensile properties obtained from the stress–strain curve are summarized in Table 3. Knitted fabric composite with $V_f = 9.5\%$, displayed elastic modulus = 5.35 GPa, tensile strength = 62.83 MPa and failure strain = 1.3%.

The elastic properties of the composite were predicted using the procedure outlined in Fig. 2 and the parameters $W = 4$ loops/2 cm, $C = 5$ loops/2 cm, $N = 20$ loops/4 cm^2 and $D_y = 1600$ Denier. The predicted elastic properties are given in Table 3. The predicted elastic modulus and Poisson ratio were approximately 20% higher than the experimental results. This may be attributed to the isostrain assumption made for estimating the elastic properties. Using an isostress assumption gives a lower estimaten of the elastic properties. In view of the irregular orientation distri-

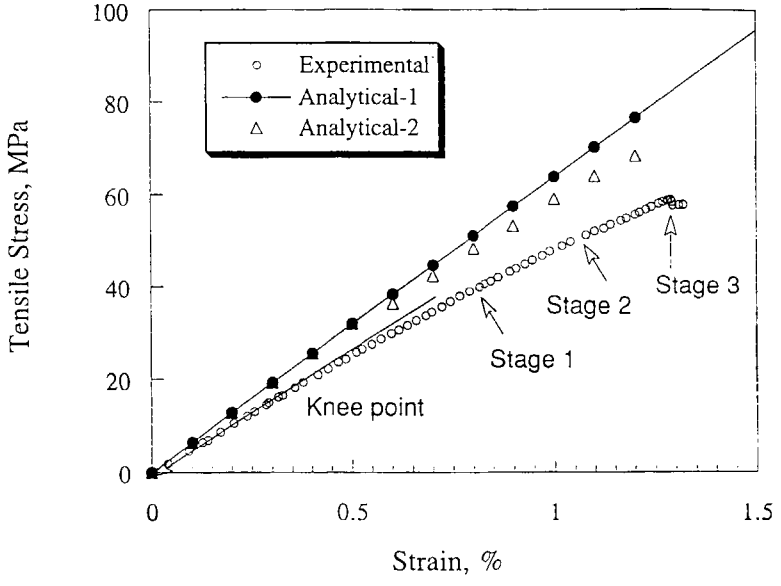

Figure 18. Tensile stress–strain curves for knitted fabric reinforced composite.

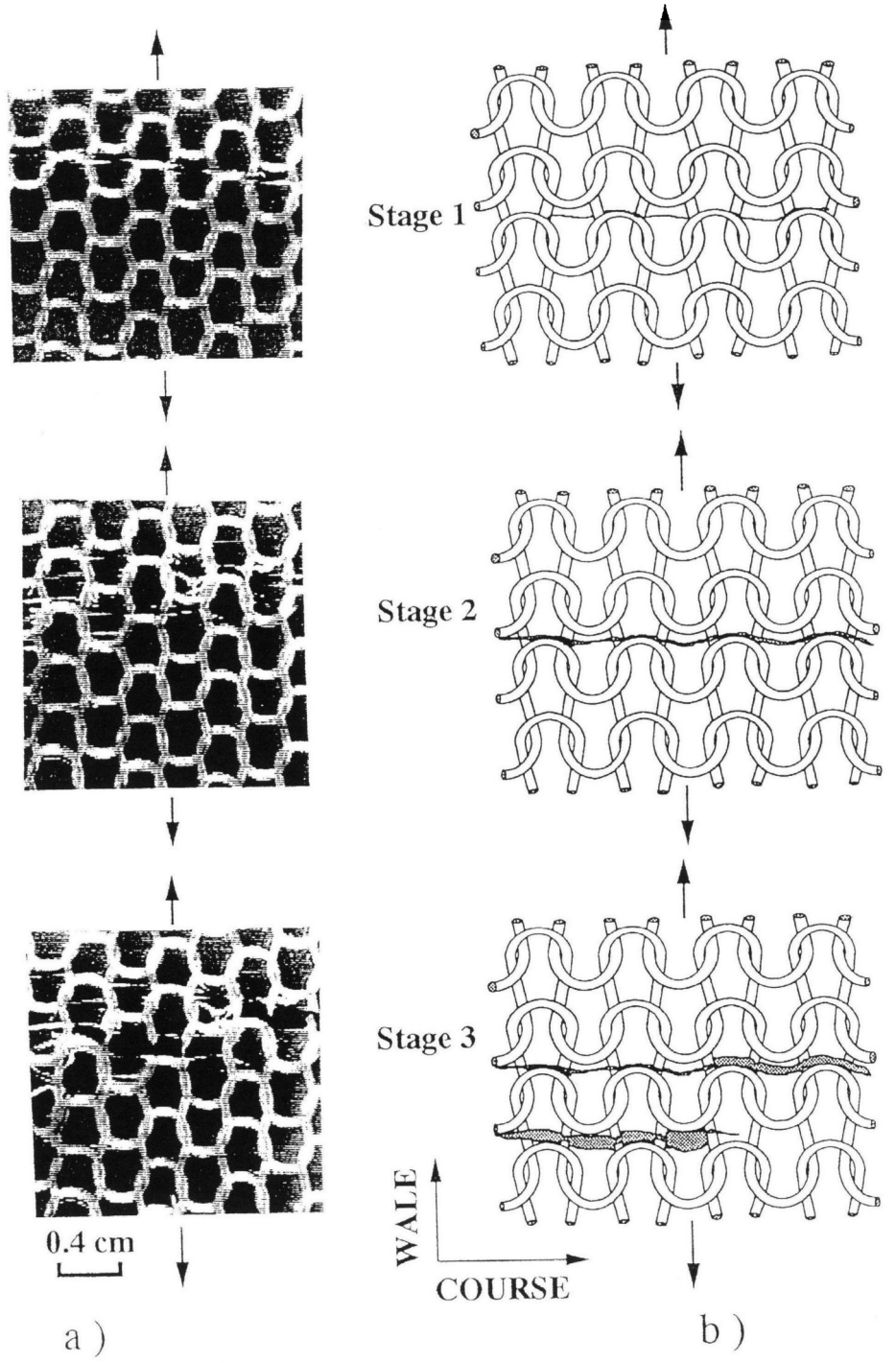

Figure 19. a) Optical photographs and b) schematic diagrams of knitted fabric composite specimen at different stages of tensile testing shown in Fig. 18.

Table 3.
Tensile properties of plain knitted glass fiber fabric/epoxy composite

	Fiber volume fraction, V_f %	Elastic modulus, E_c GPa	Poisson ratio, ν_c	Tensile strength, σ_c MPa	Ultimate failure strain %
Experimental*	9.5	5.35 (0.33)	0.48 (0.13)	62.83 (7.1)	1.3 (0.45)
Analytical	9.25	6.38	0.57	65.0	1.2

* standard deviation in brackets.

bution of fibers in a knitted fabric composite, most probably neither strain nor stress would be constant over the composite. The exact distributions of stresses and strain would depend on the local orientation of the fibers/yarn, their orientation relative to each other, and the fiber and matrix elastic properties. It is to be noted that this simplified assumption is the limitation of the present analysis. The proposed method is intended to present a preliminary and simple method of estimating elastic properties of knitted fabric composite.

Assuming a linear relationship between the stress and strain, the analytical stress–strain curve computed using estimated elastic modulus is shown in Fig. 18 (see analytical-1). At strain levels above the knee point, by incorporating the effects of microcracking of composite material, good agreement between the experimental and analytical stress–strain curves could be obtained (see experimental and analytical-2 curves in Fig. 18). The analytical-2 curve was drawn by estimating the variation of tangent modulus of the experimental curve and adjusting the analytical-1 curve accordingly. For parameters $S = 1.25$ and $\alpha_k = 15°$, predicted tensile strength was 65 MPa. The analytical failure strain corresponding to this stress was 1.2%. The analytical failure strain compare favorably with the experimental failure strain 1.3%. Using the analytical procedures developed, the tensile properties of knitted fabric reinforced composites can be predicted with reasonable accuracy.

In the present model, the projections of the central axis of the yarn bundle on the plane of the fabric were assumed to be composed of circular arcs. This may be an idealized situation. Often it is the case that the loop geometry may not be circular and suitable assumptions have to be made according to the knitted structure. The preliminary procedure outlined in this paper has to be further developed to consider the variations in the knit structure that greatly affect the composite properties.

6. CONCLUSIONS

Preliminary methodologies for predicting the tensile properties of plain knitted fabric reinforced composites have been established. The elastic properties were predicted using laminate theory and a 'cross-over model' which takes into consideration the orientation of yarns and resin-rich regions in the composite. Tensile strength properties were predicted by estimating the fracture strength of yarns bridging the fracture plane. The predicted tensile properties compare favorably with the experimental results. It is to be noted that the elastic properties were predicted by assuming uniform strain

condition and caution should be exercised in interpreting the predicted data. A more detailed analysis is necessary to assess fully the applicability and limitations of these assumptions and methods.

Tensile properties of knitted fabric composites increased with increasing fiber content. It has been shown that the fiber content of the composite can be increased by increasing a) linear density of yarn, b) stitch density of knitted fabric and c) number of plies of knitted fabrics.

Acknowledgment

The authors are grateful to Prof. K. B. Cheng of Department of Textile Engineering. National Taipei Institute of Technology, Taiwan, for his useful suggestions and technical discussions.

REFERENCES

1. Ramakrishna, S., Hamada, H., Kotaki, M., Wu, W. L., Inoda, M. and Maekawa, Z. Future of knitted fabric reinforced polymer composites. In: *Proc. of 3rd Japan International SAMPE Symposium*. Tokyo (1993), pp. 312–317.
2. Horsting, K., Wulhorst, B., Franzke, G. and Offermann, P. New types of textile fabrics for fiber composites. *SAMPLE J.* **29**, 7–12 (1993).
3. Dewalt, P. L. and Reichard, R. P. Just how good are knitted fabrics. *J. Reinf. Plast. Compos.* **13**, 908–917 (1994).
4. Ramakrishna, S., Hamada, H., Rydin, R. and Chou, T. W. Impact damage resistance of knitted glass fiber fabric reinforced polypropylene composite laminates. *Sci. Engng Compos. Mater.* **4** (2), 61–72 (1995).
5. Ramakrishna, S. and Hull, D. Energy absorption capability of epoxy composite tubes with knitted carbon fiber fabric reinforcement. *Compos. Sci. Technol.* **49**, 349–356 (1993).
6. Ramakrishna, S. Energy absorption behaviors of knitted fabric reinforced epoxy composite tubes. *J. Reinf. Plast. Compos.* **14**, 1121–1141 (1995).
7. Phillips, D. and Verpoest, I. Sandwich panels produced from 3D-knitted structures. In: *Proc. of 40th International SAMPLE Symposium*. Anaheim, California (1995), pp. 957–965.
8. Ko, F. K., Pastore, C. M., Yang, J. M. and Chou, T. W. Structure and properties of multilayer multidirectional warp knit fabric reinforced composites. In: *Proc. of 3rd Japan–US Conference*. Tokyo (1986), pp. 21–28.
9. Verpoest, I. and Dendauw, J. Mechanical properties of knitted glass fiber/epoxy resin laminates. In: *Proc. of ECCM-5*. Bordeaux (1992), pp. 927–932.
10. Gommers, B., Wang, T. K. and Verpoest, I. Mechanical properties of warp knitted fabric reinforced composites. In: *Proc. of 40th International SAMPLE Symposium*. Anaheim, California (1995), pp. 966–976.
11. Gommers, B. and Verpoest, I. Tensile behavior of knitted fabric reinforced composites. In: *Proc. of ICCM10*, Vol. IV. Vancouver (1995), pp. 309–316.
12. Rudd, C. D., Owen, M. J. and Middleton, V. Mechanical properties of weft knit glass fiber/polyester laminates. *Compos. Sci. Technol.* **39**, 261–277 (1990).
13. Chou, S., Chen, H. C. and Lai, C. C. The fatigue properties of weft-knit fabric reinforced epoxy resin composites. *Compos. Sci. Technol.* **45**, 283–291 (1992).
14. Ramakrishna, S., Fujita, A., Cuong, N. K. and Hamada, H. Tensile failure mechanisms of knitted glass fiber fabric reinforced epoxy composites. In: *Proc. of 4th Japan International SAMPLE Symposium and Exhibition*, Vol. 1. Tokyo (1995), pp. 661–666.
15. Ramakrishna, S. and Hull, D. Tensile behavior of knitted carbon-fiber-fabric/epoxy laminates – part I: Experimental. *Compos. Sci. Technol.* **50**, 237–247 (1994).

16. Ramakrishna, S. and Hull, D. Tensile behavior of knitted carbon-fiber-fabric/epoxy laminates – part II: Prediction of tensile properties. *Compos. Sci. Technol.* **50**, 249–258 (1994).
17. Ramakrishna, S., Hamada, H. and Cuong, N. K. Bolted joints of knitted fabric reinforced composites. In: *Proc. of 7th Japan–US conference*. Kyoto (1995), pp. 633–640.
18. Mayer, J., Wintermantal, E., De Angelis, F., Niedermeier, M., Buck, A. and Flemming, M. Carbon fiber knitting reinforcement (K-CF) of thermoplastics: a novel composite. In: *Proc. of Euromat.* Cambridge (1991), pp. 18–26.
19. Mayer, J., Ruffieux, K., Tognini, R. and Wintermantel, E. Knitted carbon fibers, a sophisticated textile reinforcement that offers new perspectives in thermoplastic composite processing. In: *Proc. of ECCM-6.* Bordeaux (1993), pp. 219–224.
20. Ramakrishna, S., Hamada, H. and Cuong, N. K. Fabrication of knitted glass fiber fabric reinforced thermoplastic composite laminates. *J. Adv. Compos. Lett.* **3** (6), 189–192 (1994).
21. Ramakrishna, S., Hamada, H., Cuong, N. K. and Maekawa, Z. Mechanical properties of knitted fabric reinforced thermoplastic composites. In: *Proc. of ICCM-10*, Vol. IV. Vancouver (1995), pp. 245–252.
22. Leaf, G. A. V. and Glaskin, A. The geometry of a plain knitted loop. *J. Textile Inst.*, T587–T605 (1955).
23. Ramakrishna, S. Analysis and modeling of plain knitted fabric reinforced composites. *J. Composite Materials* (in press).
24. Hearle, J. W. S., Grosberg, P. and Backer, S. *Structural Mechanics of Fibers, Yarns, and Fabrics*, p. 80. Wiley-Interscience, New York (1969).
25. Uemura, M., Ataka, N., Fukuda, H. and Ben, G. *Practical FRP Structural Strength Calculations.* Japan Society of Reinforced Plastics, Ion Publishers, Japan (1984).
26. Jones, R. M. *Mechanics of Composite Materials.* Hemisphere Publishing Corporation, USA (1975).
27. Hull, D. *An Introduction to Composite Materials*, p. 170. Cambridge University Press, UK (1981).